

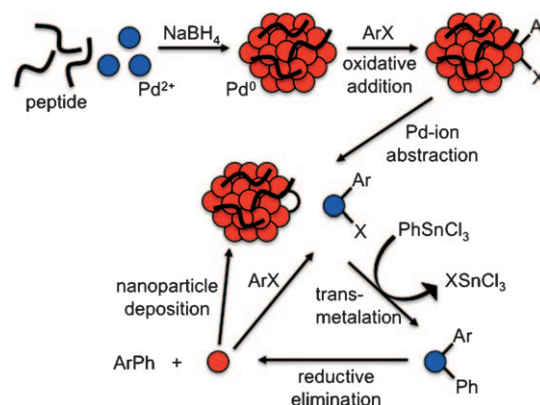
# Elucidation of Peptide Effects that Control the Activity of Nanoparticles\*\*

Ryan Coppage, Joseph M. Slocik, Manish Sethi, Dennis B. Pacardo, Rajesh R. Naik, and Marc R. Knecht\*

Natural processes have been developed to produce nanostructures that involve recognition between biomolecules and inorganic surfaces.<sup>[1]</sup> Such methods have been exploited in the production of nanomaterials for use as catalysts,<sup>[2–4]</sup> biosensors,<sup>[5]</sup> batteries,<sup>[6]</sup> and components for directed assembly;<sup>[2,7]</sup> however, the interactions at the biotic/abiotic interface remain unclear. These interactions are likely to control the activity of the nanostructures, which could be optimized based upon the peptide sequence and arrangement on the nanomaterial surface. Whilst these studies have demonstrated the unique activity of such bio-enabled materials,<sup>[2–6]</sup> to the best of our knowledge, no research is available that probes the critical effects of the surface peptide on nanomaterial activity. Previous reports have suggested that peptides bind to surfaces in a different manner to individual amino acids;<sup>[8,9]</sup> therefore, by understanding these interactions, the design of bionanomaterials that have superior functionality may be possible.

The Pd4 peptide (Table 1), was isolated using a phage display technique with an affinity for palladium.<sup>[3,9]</sup> Using this sequence, palladium particles, which have a diameter of approximately 1.9 nm, were prepared that were active for Stille coupling reactions in water, at room temperature, with

palladium loadings of  $\geq 0.005$  mol % (Scheme 1).<sup>[3]</sup> Modeling of the peptide–nanoparticle interactions suggested that the histidine residues at positions 6 and 11 were most likely



**Scheme 1.** Biomimetic synthesis and catalytic application of peptide-capped palladium nanoparticles. The Stille coupling, catalyzed by the biomimetic materials, employs an atom-leaching mechanism that is controlled by binding electronics and the arrangement of the specific peptide sequence on the nanoparticle surface during the initial oxidative addition step.

**Table 1:** Peptide sequences used to probe palladium surface effects.

Peptide	Sequence	pI <sup>[a]</sup>	Size [nm]	TOF
Pd4	TSNAVHPTLRHL	9.47	1.9 ± 0.3	2234 ± 99
A6	TSNAV <sup>A</sup> PTLRHL	9.44	2.2 ± 0.4	5224 ± 381
A11	TSNAVHPTLR <sup>A</sup> L	9.44	2.4 ± 0.5	1298 ± 107
A6,11	TSNAV <sup>A</sup> PTLR <sup>A</sup> L	9.41	3.7 ± 0.9	361 ± 21

[a] pI calculated at <http://ca.expasy.org>.

[\*] R. Coppage, M. Sethi, D. B. Pacardo, Prof. M. R. Knecht  
Department of Chemistry, University of Kentucky  
Lexington, KY 40506-0055 (USA)  
Fax: (+1) 859-323-1069  
E-mail: mrknech2@email.uky.edu

Dr. J. M. Slocik, Dr. R. R. Naik  
Nanostructured and Biological Materials Branch  
Air Force Research Laboratory  
Wright-Patterson Air Force Base, OH 45433-7702 (USA)

[\*\*] Acknowledgement is made to the Donors of the American Chemical Society Petroleum Research Fund for partial support of this research (M.K.) and the Air Force Office of Scientific Research (R.N.). Further support from the University of Kentucky is also acknowledged. We thank L. Jackson and Dr. B. Lynn for MS characterization of the peptides.

Supporting information for this article is available on the WWW under <http://dx.doi.org/10.1002/anie.200906949>.

responsible for the binding as they form a kinked structure that exposes the palladium surface.<sup>[9]</sup> Herein, we show that by selectively replacing the histidine residues with alanine, the catalytic activity can be modulated to affect the reactivity while maintaining the particle size. These results are critical in understanding the activity of biomimetic materials for two key reasons: First, they suggest that the activity of bionanomaterials can be modulated by the peptide sequence. Second, these studies highlight the underlying cause of the catalytic activity of bionanomaterials, which could be used for the rational design of peptides for the production of functional nanomaterials. Whilst the changes and enhancements in the catalytic capabilities are intriguing, the main focus of this study is to understand the activity of peptide-based materials.

The peptides used in this study were all synthesized, purified, and confirmed as previously described.<sup>[3]</sup> Four peptides were prepared (Table 1), based on the parental Pd4 sequence. These included peptides in which the histidine residues were substituted with alanine at positions 6, 11, or 6 and 11, termed A6, A11, and A6,11, respectively. For nanoparticle fabrication, each peptide was co-dissolved with 3.3 equivalents of  $K_2PdCl_4$  and allowed to sit at room temperature. After 30 minutes,  $NaBH_4$  was added to form  $Pd^0$ . No precipitation of the bulk metal was observed in any of

the cases, which suggests that all of the sequences were capable of controlling the synthesis of the palladium nanoparticles.

Initial characterization of the palladium nanoparticles was conducted using UV/Vis spectroscopy (see the Supporting Information). The spectra of the reactions prior to reduction showed an absorbance shoulder at approximately 224 nm. This absorbance is consistent with the palladium–amine ligand-to-metal charge transfer band, which indicates that  $\text{Pd}^{2+}$  binds to the peptide.<sup>[3,10]</sup> After reduction, a color change from yellow to brown was observed, with an increase in absorbance at lower wavelengths. Nearly identical spectra were noted for the materials prepared using the Pd4, A6, and A11 peptides; however, the materials prepared using the A6,11 peptide demonstrated a larger degree of scattering at longer wavelengths.

The nanoparticles obtained from the four peptides were analyzed by transmission electron microscopy (TEM; Figure 1). From this analysis, particle sizes of  $1.9 \pm 0.3$  nm,  $2.2 \pm 0.4$  nm,  $2.4 \pm 0.5$  nm, and  $3.7 \pm 0.9$  nm were observed for

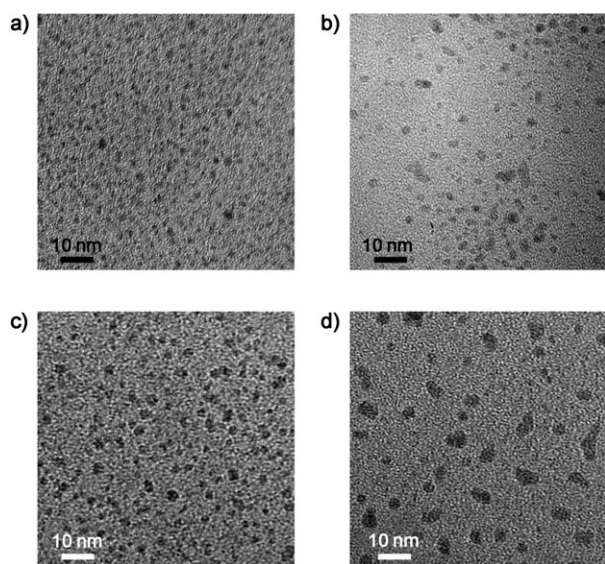


**Figure 1.** TEM images of the palladium nanoparticles prepared using the a) Pd4, b) A6, c) A11, and d) A6,11 peptides.

the materials prepared from Pd4, A6, A11, and A6,11, respectively. It is interesting that the parent Pd4 peptide generated particles that were statistically equivalent in size to those prepared from the A6 and A11 peptides, whilst the A6,11 sequence, which does not contain the predicted binding residues, results in only slightly larger particles. This indicates that the histidine residues are important for nanoparticle growth; however, their presence in the sequence is not critical. Since nanoparticles of statistically equivalent sizes were prepared when the binding residues were replaced, this suggests that the peptides are bound to the nanoparticle surface in different orientations. Indeed, CD spectra (Figure 2) of the prepared nanoparticles<sup>[11]</sup> demonstrated altered peptide motifs on the surface, based upon the modifications in the sequence. Collectively, peptides Pd4,

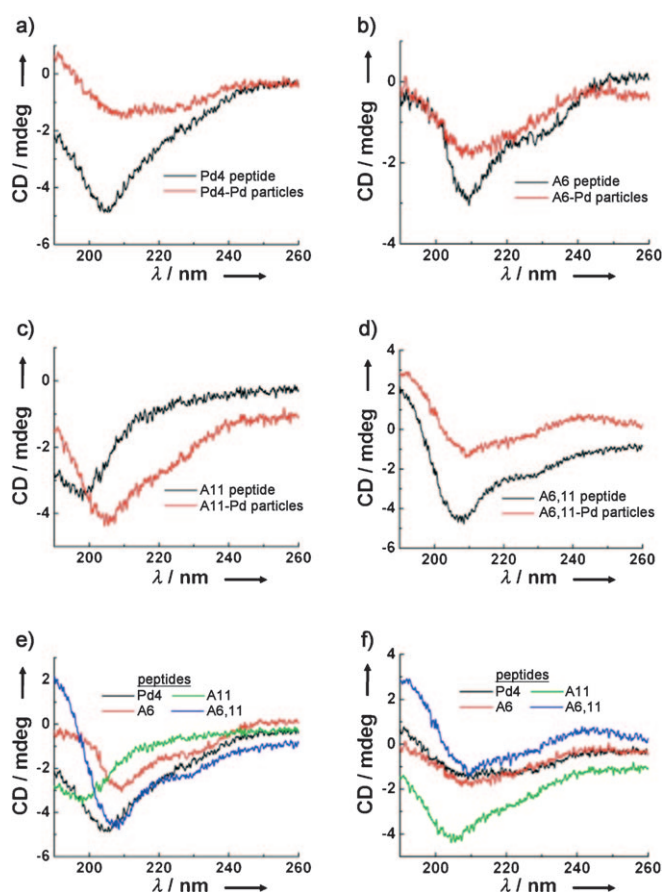


**Figure 2.** Circular dichroism (CD) spectra of the peptides and the peptide-capped palladium nanoparticles prepared using the a) Pd4, b) A6, c) A11, and d) A6,11 peptides. e) Comparison of the free peptides in solution. f) CD spectra for the different palladium nanoparticles.

A6, and A6,11 became less structured when bound to the nanoparticle surface, as shown by a decrease in ellipticity; whereas the A11 peptide became more helical relative to the free peptides (Figure 2a–d). Notably, the free peptides of A6,11 and A6 adopted an  $\alpha$ -helical structure, whilst A11 and Pd4 adopted random coil and mostly  $3_{10}$  helix structures, respectively (Figure 2e); however, on binding to the nanoparticle surface, the A11 peptide became more ordered, while Pd4 and A6 shared similar secondary structures with subtle differences.

Stille coupling reactions were conducted on the palladium nanoparticles using a modified procedure.<sup>[3,12]</sup> In each reaction, 0.25 mmol of 4-iodobenzoic acid was dissolved in 4.0 mL of 2.25 M KOH.  $\text{PhSnCl}_3$  (0.30 mmol) was added to the mixture to generate biphenylcarboxylic acid (BPCA). The nanoparticles were then added at concentrations of  $< 0.5$  mol % palladium and the mixture was stirred for 24 hours at room temperature. Upon completion, the reactions were quenched and the products were quantified.

Analysis of the palladium loading as a function of product yield is presented in Figure 3a. The native Pd4 peptide demonstrated quantitative yields in 24 hours at a palladium loading of 0.005 mol %, consistent with previous results.<sup>[3]</sup>

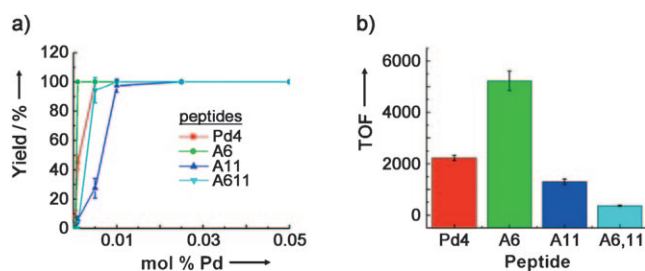


**Figure 3.** Effect of the different peptides on the reactivity of the nanocatalyst for a) palladium loading versus product yield and b) turnover frequency (TOF; y-axis units = mol BPCA (mol Pd)<sup>-1</sup> h<sup>-1</sup>).

Analysis of the material prepared with the A6 peptide found that the loading to achieve quantitative yield shifted to 0.001 mol %. Interestingly, with the other nanoparticles passivated with the A11 and A6,11 peptides, higher catalyst loadings of 0.01 mol % palladium were required for the reaction to reach completion in 24 hours.

Studies probing the turnover frequency (TOF) of the four systems were also performed. For these studies, the reactions were scaled up and then aliquots were extracted and quantified at various time intervals; the average of triplicate samples are shown in Figure 3b. For the materials prepared using the Pd4 peptide, a TOF value of  $2234 \pm 99$  mol BPCA (mol Pd)<sup>-1</sup> h<sup>-1</sup> was observed. The TOF values are calculated using the total palladium concentration, consistent with previous studies.<sup>[12–14]</sup> A TOF of 2234 is slightly lower than previously reported;<sup>[3]</sup> this is likely due to changes in the reaction conditions. Surprisingly, analysis of the A6-based materials demonstrated a TOF of  $5224 \pm 381$  mol BPCA (mol Pd)<sup>-1</sup> h<sup>-1</sup>, which corresponds to a greater-than-twofold increase in reactivity. When the A11 sample was probed, a decrease in the TOF was observed to  $1298 \pm 107$  mol BPCA (mol Pd)<sup>-1</sup> h<sup>-1</sup>, which was further decreased to  $361 \pm 21$  mol BPCA (mol Pd)<sup>-1</sup> h<sup>-1</sup> for the A6,11-derived nanoparticles.

The catalysis and TEM data suggest that the peptide sequence on the particle surface controls both the structure and reactivity of the palladium nanoparticles. The Pd4 sequence was optimized for palladium surface binding, which has been suggested to occur mainly through the histidine residues.<sup>[9]</sup> Alanine substitution of either of the histidine units demonstrated minimal changes in particle size, within the error of the measurement, which indicates that other amino acids in the sequence, asparagine and arginine, may be involved in surface binding to maintain the particle size and stability. When both histidine residues are replaced with alanine, the particle size marginally increased, which also supports binding through the other residues. Once the nanoparticles are decorated with the different sequences on the surface, different conformations and arrangements are possible based upon the individual binding capabilities. As such, changes to the palladium surface may occur, which could result in the different degrees of catalytic reactivity observed. This theory is supported by the CD spectra of the different peptides on the nanoparticle surface, which adopted different structures based upon the individual sequence.

The catalytic reactivity of the biomimetic materials likely follows an atom-leaching mechanism (Scheme 1); during the initial oxidative addition step, Pd<sup>2+</sup> is abstracted from the surface to drive the reaction, which is controlled by the peptides.<sup>[13–15]</sup> Under this process, as discussed by Astruc and co-workers, if the peptides played no role in the reactivity, regardless of slight particle size differences, the TOF values should be constant for the different particles;<sup>[13,14]</sup> however, they are drastically different, which suggests that the surface peptides modulate the reactivity. For instance, when dendrimer-based palladium nanoparticles of similar sizes to the peptide-capped particles were used, equivalent TOF values were observed, which is attributed to the lack of involvement of the dendrimer passivant in the reaction.<sup>[13,14]</sup> For the biomimetic materials, the peptide sequence is critically important to the overall TOF value. The replacement of histidine at position 6 improves the catalytic activity while histidine at position 11 is required for generating highly reactive nanoparticles. Furthermore, since nanoparticles of similar sizes were prepared, the number of moles of surface palladium atoms is similar, thus suggesting that the major difference between the particles is the biotic/abiotic interface, which is controlled by different peptide binding motifs. As the atom-leaching method would likely alter particle morphologies, we attempted to observe the materials by using TEM after the reaction. Unfortunately, at the very dilute nanocatalyst concentrations that were employed in these reactions, we were unable to observe any nanoparticles on the TEM grid. From this, two peptide-mediated events are possible to modulate the ability to abstract palladium atoms from the nanoparticle surface: First, the surface structure may be such that the orientation of the A6 peptide maximally exposes the palladium surface, thus enhancing the initial oxidative addition step and releasing Pd<sup>2+</sup> faster. As a result, more palladium would react in a shorter time to result in higher TOF values. Second, by removal of specific histidine residues, other residues are likely to bind to the surface to maintain particle stability. As such, the electronic character of the palladium surface could vary based upon the individual binding, which is known to inhibit the initial oxidative addition at the particle surface.<sup>[13]</sup> This would result in varied TOF values as a function of the electronic effects of the binding motifs of the peptides. At present, we are unable to fully distinguish between these events; however, both are controlled by the peptide.

In summary, we have demonstrated significant modulations in the reactivity of biomimetic nanomaterials by subtle modifications to the peptide sequence. This suggests that the peptide and its binding effects control the functionality of the nanomaterials. Peptides that are isolated by phage display<sup>[1]</sup> are optimized for binding. Whilst this is useful for structural stability, such attributes may cause a decrease in activity. The results presented here indicate that by altering the sequence, particle stability may be maintained with desirable increases in nanoparticle reactivity, which could be used as a basis for the rational design of optimized peptide sequences.

Received: December 9, 2009

Published online: April 15, 2010

**Keywords:** bionanotechnology · heterogeneous catalysis · nanoparticles · palladium · peptides

- [1] M. B. Dickerson, K. H. Sandhage, R. R. Naik, *Chem. Rev.* **2008**, *108*, 4935.
- [2] J. M. Slocik, A. O. Govorov, R. R. Naik, *Angew. Chem.* **2008**, *120*, 5415; *Angew. Chem. Int. Ed.* **2008**, *47*, 5335.
- [3] D. B. Pacardo, M. Sethi, S. E. Jones, R. R. Naik, M. R. Knecht, *ACS Nano* **2009**, *3*, 1288.
- [4] J. M. Slocik, R. R. Naik, *Adv. Mater.* **2006**, *18*, 1988.
- [5] J. M. Slocik, J. S. Zabinsky, D. M. Phillips, R. R. Naik, *Small* **2008**, *4*, 548.
- [6] a) Y. J. Lee, H. Yi, W.-J. Kim, K. Kang, D. S. Yun, M. S. Strano, G. Ceder, A. M. Belcher, *Science* **2009**, *324*, 1051; b) K. T. Nam, D.-W. Kim, P. J. Yoo, C.-Y. Chiang, N. Meethong, P. T. Hammond, Y.-M. Chiang, A. M. Belcher, *Science* **2006**, *312*, 885.
- [7] C.-L. Chen, P. Zhang, N. L. Rosi, *J. Am. Chem. Soc.* **2008**, *130*, 13555.
- [8] a) C. R. So, J. L. Kulp, E. E. Oren, H. Zareie, C. Tamerler, J. S. Evans, M. Sarikaya, *ACS Nano* **2009**, *3*, 1525; b) M. Sethi, M. R. Knecht, *ACS Appl. Mater. Interfaces* **2009**, *1*, 1270.
- [9] R. B. Pandey, H. Heinz, J. Feng, B. L. Farmer, J. M. Slocik, L. F. Drummy, R. R. Naik, *Phys. Chem. Chem. Phys.* **2009**, *11*, 1989.
- [10] M. R. Knecht, M. G. Weir, A. I. Frenkel, R. M. Crooks, *Chem. Mater.* **2008**, *20*, 1019.
- [11] I. Olmedo, E. Araya, F. Sanz, E. Medina, J. Arbiol, P. Toledo, A. Álvarez-Lueje, E. Giralt, M. J. Kogan, *Bioconjugate Chem.* **2008**, *19*, 1154.
- [12] J. C. Garcia-Martinez, R. Lezutekong, R. M. Crooks, *J. Am. Chem. Soc.* **2005**, *127*, 5097.
- [13] A. K. Diallo, C. Ornelas, L. Salmon, J. R. Aranzaes, D. Astruc, *Angew. Chem.* **2007**, *119*, 8798; *Angew. Chem. Int. Ed.* **2007**, *46*, 8644.
- [14] C. Ornelas, J. Ruiz, L. Salmon, D. Astruc, *Adv. Synth. Catal.* **2008**, *350*, 837.
- [15] D. Astruc, *Inorg. Chem.* **2007**, *46*, 1884; N. T. S. Phan, M. Van Der Sluys, C. W. Jones, *Adv. Synth. Catal.* **2006**, *348*, 609.